

Circumnavigating a Moving Target with Range-only Measurements

Fei Dong, Keyou You, *Senior Member, IEEE*, Lihua Xie, *Fellow, IEEE*

Abstract—This paper designs a novel coordinate-free controller for an underactuated pursuer to circumnavigate a fully actuated target with *range-only* measurements. If the range rate is further available, the controller has a simple PD-like form with a bias to eliminate steady-state circumnavigating error. In particular, such a controller drives the circumnavigating error to zero with an exponential convergence speed if the target is stationary, and otherwise to a small region whose size is explicitly proportional to the maximum speed and acceleration of the moving target. To access the range rate, we design a second-order sliding mode (SOSM) filter and show that the SOSM filter can exactly recover the range rate in a finite time. Thus, the above convergence results can be easily achieved even without the explicit range rate. Finally, the effectiveness and advantages of the proposed controller are validated via simulations.

Index Terms—Circumnavigation, range-only measurements, PD-like controller, SOSM filter.

I. INTRODUCTION

Target circumnavigation requires a pursuer to enclose a target with a desired radius to neutralize the target by restricting its movement [1], [2]. This formation has been widely applied in both military and civilian fields, such as path following [3], [4], source seeking [5], environmental boundaries monitoring [6], and etc. In Table I, we categorize the existing methods for the target circumnavigation problem by the availability of the state information of the pursuer and the target.

If the states (position, velocity, course, etc.) of both the pursuer and target are available, a Lyapunov guidance vector fields (LGVF) method is proposed in [7] and then extended in [8], [9]. Moreover, different vector field methods are proposed for the circular orbit tracking in [10]–[12].

For an uncooperative target, its state is unknown to the pursuer. To complete the circumnavigation task, the challenge is how to estimate the target state with sensor measurements, such as range-based [1], [13]–[15], bearing-based [16], [17], or received signal strength-based [18]. For a stationary target, an adaptive localization algorithm is devised using range-only measurements in [1]. A discrete-time observer is given in [19] by using the range and range-rate measurements. For a moving target, an adaptive motion estimator, an extended Kalman filter and a Rao-Blackwellised particle filter are exploited in [3],

[20] and [9], respectively. However, it is impossible to locate the target if the pursuer state is further unavailable.

If neither the pursuer state nor the target state is available, e.g., the pursuer travels in underwater or indoor environments, a range-based controller is designed in [21], [22], the parameters of which are defined by the maximum range of the controller operating space. Moreover, Cao introduces a geometrical guidance law in [23], whose idea is to drive the pursuer towards a tangent point of an auxiliary circle. However, the control input is set as zero when the pursuer enters this auxiliary circle, which may result in large overshoot. To fix it, Zhang *et al.* provides a revised version in [24]. However, their control input is also switched on the basis of the circumnavigating error. It is worth mentioning that all range-based controllers mentioned above are concerned with the problem of *stationary* target circumnavigation. It is unclear whether their methods can be extended to the case of a moving target.

It is no doubt that circumnavigating a moving target is more practical and significant. To this end, a sliding mode approach is proposed in [2], [25], [26]. To eliminate the chattering phenomenon, they model the dynamics of the actuator as the simplest first-order linear differential equation [27]. However, their approach cannot achieve zero steady-state error, even for a *stationary* target. Besides, it requires the pursuer to start far from the target. The authors in [28] devise a stochastic approach by further using relative angles to solve their optimal control problem. Shames *et al.* show that the upper bound of the circumnavigating error is proportional to the maximum linear speed of the moving target in [1], which however is a coordinate-based¹ method. In contrast, we obtain the same results only using the range measurements.

In some scenarios, the range rate may be inaccessible to the pursuer due to the limited sensing capability of small robots. Moreover, it is ineffective to calculate the range rate by differentiating methods using range measurements, since even small noises may result in large or unbounded estimation errors. To address it, a first-order filter and a washout filter are adopted in [29] and [30], respectively. However, there is no rigorous justification of the first-order filter. Moreover, a second-order sliding mode (SOSM) filter is proposed in [31] and is adopted for solving the stationary target circumnavigation problem in [23]. It is more difficult to estimate the range rate when both the speed and acceleration of the target are time-varying.

We propose a coordinate-free controller on the basis of

¹The word “Coordinate-based” (“Coordinate-free”) implies that the controller is designed with (without) the position of the pursuer.

This work was supported in part by the National Natural Science Foundation of China under Grant 61722308. (*Corresponding author: Keyou You*)

F. Dong and K. You are with the Department of Automation, and Beijing National Research Center for Info. Sci. & Tech. (BNRist), Tsinghua University, Beijing 100084, China. E-mail: dongf17@mails.tsinghua.edu.cn, youky@tsinghua.edu.cn.

L. Xie is with the School of Electrical and Electronic Engineering, Nanyang Technological University, Singapore 639798, Singapore. E-mail: elhxie@ntu.edu.sg.

TABLE I
SUMMARY OF EXISTING METHODS FOR TARGET CIRCUMNAVIGATION

Pursuer state	Target state	Method
Yes	Yes	Lyapunov guidance vector fields [7]–[9]
		Vector-Field-Orientation [10]
		Orbital guidance strategy [11]
		Guiding vector-field algorithm [12]
Yes	No	Adaptive localization algorithm [1]
		Adaptive motion estimator [3]
		Extended Kalman filter [20]
		Rao-Blackwellised particle filter [9]
		Discrete-time observer [19]
		Projection estimator [32]
No	No	Range-based feedback controller [21], [22]
		Geometrical guidance law [23]
		Switching controller [24]
		Sliding mode controller [2], [25], [26]

our preliminary work [33] to ensure that the pursuer can circumnavigate a moving target with a prescribed radius by using range-only measurements. The proposed controller in this paper also differs from the one in our previous work [34], which aims at steering the pursuer to follow a smooth reference command. Given that the target is stationary and both range and range rate measurements are known, our controller can guarantee global convergence and local exponential stability. This implies that the closed-loop system is robust against perturbations [35, Section 9.2]. Then, we explicitly show the upper bound of the circumnavigating error, which is proportional to the maximum linear speed and acceleration of the target. This is consistent with the results of [1], which steers a single-integrator pursuer and requires its own position. For a specific target and pursuer, we can reduce this error bound by selecting proper control parameters. Note that the selection of the control parameters is independent of the initial state by means of the saturation function. Finally, we revise our controller into a range-only form by replacing the actual range rate with its estimated version by design an SOSM filter. We show that the convergence time is finite if the initial distance to the target is sufficiently large and both the speed and acceleration of the target are bounded.

The rest of this paper is organized as follows. In Section II, the problem under consideration is formulated in details where we explicitly define the target circumnavigation problem. In Section III, two PD-like controllers are proposed depending on whether the explicit range rate is known or not. For the case where the explicit range-rate is known, we show the global convergence and local exponential stability of the proposed controller in Section IV, and further prove that the circumnavigating error is bounded when the target is moving. Moreover, target circumnavigation without explicit range rate is studied in Section V. Simulations are performed in Section VI, and some concluding remarks are drawn in Section VII.

II. PROBLEM FORMULATION

In Fig. 1, we have a fully actuated moving target on a plane

$$\dot{\mathbf{p}}_o(t) = \mathbf{v}_o(t), \quad \dot{\mathbf{v}}_o(t) = \mathbf{a}_o(t), \quad (1)$$

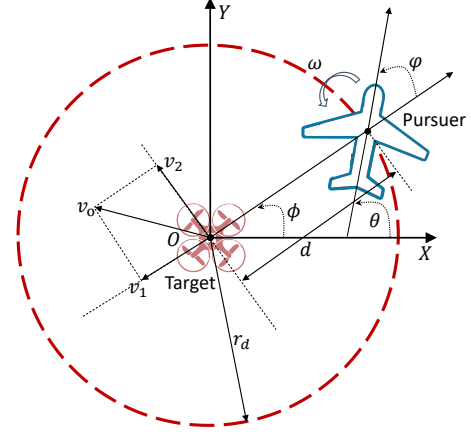


Fig. 1. Circumnavigation of a moving target.

and an underactuated pursuer

$$\begin{aligned} \dot{\mathbf{p}}(t) &= [v \cos \theta(t), v \sin \theta(t)]', \\ \dot{\theta}(t) &= \omega(t), \end{aligned} \quad (2)$$

where $\mathbf{p}_o(t)$, $\mathbf{v}_o(t)$, $\mathbf{a}_o(t) \in \mathbb{R}^2$ denote the position, linear velocity, acceleration of the target, and $\mathbf{p}(t) \in \mathbb{R}^2$, $\theta(t)$, $\omega(t)$, v are the position, heading course, angular speed, constant linear velocity of the pursuer over the plane, respectively. It is worth mentioning that the target and the pursuer may travel with different altitudes, e.g., a fixed-wing UAV tracks a ground moving vehicle where Fig. 1 denotes the projection of the real 3D trajectory of the pursuer to the 2D plane. In this work, we can only take the range measurement from the pursuer to the target, i.e.,

$$d(t) = \|\mathbf{p}(t) - \mathbf{p}_o(t)\|_2.$$

Neither the target position or the pursuer position is accessible. This is very useful for a notable example is that the pursuer travels in GPS-denied environments and the target is a non-cooperative intruder.

Our goal is to design a coordinate-free controller with range-only measurements to drive the pursuer (2) to circumnavigate the target (1) with a predefined radius r_d . Mathematically,

- (i) if $\mathbf{p}_o(t) \equiv \mathbf{p}_o$ is constant, it holds that

$$\lim_{t \rightarrow \infty} |d(t) - r_d| = \lim_{t \rightarrow \infty} |\dot{d}(t)| = 0. \quad (3)$$

- (ii) if both $\|\mathbf{v}_o(t)\|_2 \leq \bar{v}_o$ and $\|\mathbf{a}_o(t)\|_2 \leq \bar{a}_o$ for all $t \geq t_0$, there is a constant κ such that

$$\limsup_{t \rightarrow \infty} |d(t) - r_d| \leq \kappa, \quad (4)$$

where κ is proportional to \bar{v}_o and \bar{a}_o .

That is, the trajectory of the pursuer onto the plane in (3) is expected to form an exact circle with the unknown target position \mathbf{p}_o and r_d as its center and radius. In (4), the trajectory is close to a circle with $\mathbf{p}_o(t)$ and r_d as its moving center and radius, the derivation of which is proportional to the maximum speed and acceleration of the moving target. The requirement that $\bar{v}_o < v$ is natural as the target should not be faster than the pursuer.

In [1], the two objectives in (3) and (4) have also been simultaneously achieved for a single-integrator pursuer by further using its own exact position information, which is essential to their controller design. While in this work, we show it is not necessary without sacrificing the final circumnavigating performance.

III. CONTROLLER DESIGN

To achieve the objectives in (3) and (4), we propose two controllers. (i) The first is the range-based controller in (6) by using both the range and range rate measurements. It has a simple PD-like form with a bias to eliminate the steady-state circumnavigating error. A similar idea has been presented in our preliminary work [33], which however only investigates the case of a stationary target with the explicit range rate feedback. (ii) The second is the range-only controller in (9) by further designing an SOSM filter to perfectly recover the range rate if both the linear speed and acceleration of the target are bounded.

A. The PD-like controller with explicit range rate

To solve the circumnavigation problem, define the relative tracking error and a saturation function as

$$e(t) = \frac{d(t) - r_d}{r_d} \text{ and } \text{sat}(z) = \begin{cases} z, & \text{if } |z| < 1, \\ \text{sgn}(z), & \text{if } |z| \geq 1, \end{cases} \quad (5)$$

where $\text{sgn}(\cdot)$ is the standard sign function.

If the range rate $\dot{d}(t)$ is perfectly known, we propose a novel PD-like range-based controller

$$\omega(t) = \omega_c + c_1 \dot{e}(t) + c_2 \text{sat}(e(t)), \quad (6)$$

where c_i is a positive parameter to be designed and $\omega_c = v/r_d$ is a bias to eliminate the steady-state circumnavigating error. For example, if $d(t) = r_d$ and $\dot{d}(t) = 0$ at some time t , then $\omega(t) = \omega_c$ is the desired angular speed of the pursuer, and if the target is stationary, the pursuer will keep this angular speed all the time. The major difference from the standard PD controller lies in the use of a saturation function to ensure that the control parameters can be selected *independently* of the initial states of the circumnavigation system. As the system is inherently nonlinear, one cannot expect to use a linear controller to complete the circumnavigation task. From this perspective, our controller is the “simplest” one.

If the target is stationary, we show later in Proposition 1 that the range-based controller in (6) can even achieve an exponential convergence with a fix set of parameters for any initial condition. In comparison, the sliding mode approach in [2] requires that the initial range to the target $d(t_0)$ is sufficiently larger than the desired radius r_d , and their controller cannot achieve exact circumnavigation even for the case of a stationary target, i.e., $e(t)$ cannot exactly converge to zero. The geometrical method in [23] uses a pair of a trigonometric function and an inverse trigonometric function to drive the pursuer towards the tangent point of an auxiliary circle, and there is no control input when the pursuer enters this auxiliary circle, which may result in large overshoot. Moreover, the

control parameters in [22] are determined by the maximum range of the controller operating space. In [34], we have studied the closely related target encirclement problem under any smooth pattern. Importantly, all the aforementioned controllers are only concerned with the case of a stationary target, and it is unclear whether their controllers can be extended to the case of a moving target. Overall, our controller in (6) not only has a simpler form but also can be used to circumnavigate a moving target.

Since the controller of this work only uses the range-based measurements between the pursuer and target, it is particularly useful in GPS-denied environments and also substantially different from [3], [16], [20], [36] as they need the pursuer position.

B. The PD-like controller without explicit range rate

If the range rate $\dot{d}(t)$ is unknown and note that it is ineffective to directly compute it by the differentiating method, we design an SOSM filter [31] to estimate it, i.e.,

$$\begin{aligned} \dot{\alpha}_1(t) &= k_1 |d(t) - \alpha_1(t)|^{1/2} \text{sgn}(d(t) - \alpha_1(t)) \\ &\quad + k_2 (d(t) - \alpha_1(t)) + \alpha_2(t), \\ \dot{\alpha}_2(t) &= k_3 \text{sgn}(d(t) - \alpha_1(t)) + k_4 (d(t) - \alpha_1(t)), \end{aligned} \quad (7)$$

where k_i is a positive filter parameter to be designed. If both the linear speed and acceleration of the target are bounded, we show later that there is a finite time T satisfying

$$d(t) - \alpha_1(t) = \dot{d}(t) - \alpha_2(t) = 0, \quad \forall t \geq t_0 + T. \quad (8)$$

Thus, we directly replace $\dot{e}(t)$ in (6) by $\alpha_2(t)/r_d$ and obtain the following range-only controller

$$\omega(t) = \omega_c + c_1/r_d \cdot \alpha_2(t) + c_2 \text{sat}(e(t)). \quad (9)$$

IV. MOVING TARGET CIRCUMNAVIGATION UNDER THE RANGE-BASED CONTROLLER

If the target is stationary, we show in Proposition 1 that the range-based controller in (6) can achieve an exponential convergence with a fix set of parameters for any initial condition. Otherwise, we show in Proposition 2 that the upper bound of the circumnavigating error is explicitly proportional to the maximum linear speed and acceleration of the moving target.

A. The Stationary Target Circumnavigation

For a stationary target, i.e., $\bar{v}_o = 0$, let \mathbf{p}_o be the *unknown* position of the target. Consider a polar frame centered at the target, we convert the dynamics in (2) from the Cartesian coordinates into the following form

$$\begin{aligned} \dot{d}(t) &= v \cos \varphi(t), \\ \dot{\varphi}(t) &= \omega(t) - \frac{v}{d(t)} \sin \varphi(t), \end{aligned} \quad (10)$$

where the angle $\varphi(t) \in (-\pi, \pi]$ is formed by the direction that the target points to the pursuer and the heading direction of the pursuer, see Fig. 1. By convention, the counter-clockwise

direction is set to be positive. From Fig. 1, we also have the following relationship

$$\varphi(t) = \theta(t) - \phi(t),$$

where $\phi(t)$ is formed by the direction from the target to the pursuer and the positive direction of x -axis. By Fig. 1, one can easily observe that $d(t) = r_d$ and $\varphi(t) = \pi/2$ is the desired circumnavigation, which is also the equilibrium of (10).

Now, we show that the closed-loop system (10) with the range-based controller in (6) is asymptotically stable with an exponential convergence speed.

Proposition 1: Consider the circumnavigation system in (10) under the PD-like controller in (6). Let $\mathbf{x}(t) = [d(t), \varphi(t)]'$ and $\mathbf{x}_e = [r_d, \pi/2]'$. If the parameters of the controller are selected to satisfy that

$$(c_1 - 1)\omega_c > c_2, \quad (11)$$

there exists a finite $t_1 \geq t_0$ such that

$$\|\mathbf{x}(t) - \mathbf{x}_e\| \leq C\|\mathbf{x}(t_1) - \mathbf{x}_e\| \exp(-\rho(t - t_1)), \forall t > t_1,$$

where ρ and C are two positive constants.

Proof: See Appendix A. ■

It is clear that the convergence speed to the equilibrium is exponentially fast. Thus, arbitrarily small perturbations will not result in large steady-state deviations from the equilibrium [35, Section 9.2]. Moreover, the selection of control parameters $c_i, i = 1, 2$ is independent on $d(t_0)$. Our circumnavigation objective is eventually achieved in the sense of (3).

B. The Moving Target Circumnavigation

If the target is moving, we decompose its forward velocity $\mathbf{v}_o(t)$ into $v_1(t)$ and $v_2(t)$, which denote the radial and tangential velocities of the target relative to the pursuer, respectively. See Fig. 1 for illustrations. Then the dynamics between the pursuer and the target is given by

$$\begin{aligned} \dot{d}(t) &= v \cos \varphi(t) - v_1(t), \\ \dot{\varphi}(t) &= \omega(t) - \frac{v}{d(t)} \sin \varphi(t) + \frac{v_2(t)}{d(t)}, \end{aligned} \quad (12)$$

where

$$\begin{aligned} \dot{\varphi}(t) &= \omega(t) - \dot{\phi}(t), \\ \dot{\phi}(t) &= \frac{v \sin \varphi(t) - v_2(t)}{d(t)}. \end{aligned}$$

Now, we show that the circumnavigating error of the closed-loop system (12) with the PD-like controller (6) is bounded by a constant, which is proportional to the maximum linear speed and acceleration of the target. This is also validated by the simulations in Section VI-B. Moreover, we can reduce the upper bound of the circumnavigating error by properly increasing $c_i, i = 1, 2$, with satisfying the conditions in Proposition 2.

Proposition 2: Consider the target circumnavigation system in (12) under the range-based controller in (6). If $\|\mathbf{v}_o(t)\|_2 \leq$

$\bar{v}_o, \|\mathbf{a}_o(t)\|_2 \leq \bar{a}_o$, and the parameters of the controller are selected to satisfy that

$$\begin{aligned} (c_1 - 1)\omega_c &> c_2 + (c_1 + 1)\omega_o, \\ c_2 &> \max((c_1 + 1)\omega_o, 2\omega_c + 4\omega_o), \end{aligned}$$

where $\omega_o = \bar{v}_o/r_d$, there are finite $\kappa > 0$ of the form

$$\kappa = \mathcal{O}\left(\frac{v + \bar{v}_o + \bar{a}_o}{c_2} + \frac{v + \bar{v}_o}{c_1}\right) \quad (13)$$

and $T_1 > 0$ such that $\limsup_{t \rightarrow \infty} |d(t) - r_d| \leq \kappa$ for all $d(t_0) > 2r_d + (v + \bar{v}_o)T_1$.

Proof: Let

$$z(t) = \dot{e}(t) + c_2/c_1 \cdot \text{sat}(e(t)). \quad (14)$$

Firstly, we show the uniform boundedness of $z(t)$, which together with Lemma 2 of [2] implies that $e(t)$ is also uniformly bounded. To this end, consider a Lyapunov function candidate

$$V_z(z) = \frac{1}{2}z^2(t).$$

If $d(t) \geq 2r_d$, it follows from (6) and (12) that

$$\begin{aligned} \dot{z}(t) &= -c_1\omega_c z(t) \sin \varphi(t) \\ &\quad - \left(\omega_c - \frac{v}{d(t)} \sin \varphi(t) + \frac{v_2(t)}{d(t)}\right) \omega_c \sin \varphi(t) + \frac{\dot{v}_1(t)}{r_d}. \end{aligned}$$

Thus, we have that

$$\begin{aligned} \dot{V}_z(z) &= -z^2(t)c_1\omega_c \sin \varphi(t) - z(t) \times \\ &\quad \left(\left(\omega_c - \frac{v \sin \varphi(t)}{d(t)} + \frac{v_2(t)}{d(t)}\right) \omega_c \sin \varphi(t) + \frac{\dot{v}_1(t)}{r_d}\right) \\ &< -z^2(t)c_1\omega_c \sin \varphi(t) + |z(t)| \left(\omega_c(\omega_c + \omega_o) + \frac{\bar{a}_o}{r_d}\right). \end{aligned} \quad (15)$$

If $d(t) \in (r_d/2, 2r_d)$, it similarly holds that

$$\begin{aligned} \dot{V}_z(z) &= -z^2(t)c_1\omega_c \sin \varphi(t) - z(t) \times \\ &\quad \left(\left(\omega_c - \frac{v \sin \varphi(t)}{d(t)} + \frac{v_2(t)}{d(t)}\right) \omega_c \sin \varphi(t) + \frac{\dot{v}_1(t)}{r_d} + \frac{c_2}{c_1} \dot{e}(t)\right) \\ &< -z^2(t)c_1\omega_c \sin \varphi(t) \\ &\quad + |z(t)| (\omega_c(\omega_c + 2\omega_o) + \bar{a}_o/r_d + c_2(v + \bar{v}_o)/c_1). \end{aligned} \quad (16)$$

In light of (15) and (16), if $d(t) > r_d/2$ and $\sin \varphi(t) \geq \sin \varphi_*$, where $\sin \varphi_*$ is to be given in (19), it implies that

$$\begin{aligned} \dot{V}_z(z) &< -c_1\omega_c z^2(t) \sin \varphi_* \\ &\quad + |z(t)| (\omega_c(\omega_c + 2\omega_o) + \bar{a}_o/r_d + c_2(v + \bar{v}_o)/c_1). \end{aligned}$$

Thus, $\dot{V}_z(z) < 0$ holds for all

$$|z(t)| \geq \frac{\kappa_1}{c_1} = \frac{\omega_c(\omega_c + 2\omega_o) + \bar{a}_o/r_d + c_2(v + \bar{v}_o)/c_1}{c_1 \cdot \omega_c \sin \varphi_*}.$$

This implies that $|z(t)|$ will be bounded by κ_1/c_1 .

Together (14) and Lemma 2 of [2], it eventually holds that

$$\lim_{t \rightarrow \infty} |d(t) - r_d| \leq \kappa = \kappa_1 r_d / c_2,$$

where

$$\kappa = \frac{v + 2\bar{v}_o}{c_2 \sin \varphi_*} + \frac{\bar{a}_o}{c_2 \omega_c \sin \varphi_*} + \frac{r_d(v + \bar{v}_o)}{c_1 \omega_c \sin \varphi_*}. \quad (17)$$

Then, we show that there exists a finite $t_1 \geq t_0$ such that $\sin \varphi(t) \geq \sin \varphi_* > 0$ for all $t \geq t_1$. Inserting (6) into (12) leads to that

$$\dot{\varphi}(t) = c_1 z(t) + v/r_d - v/d(t) \cdot \sin \varphi(t) + v_2(t)/d(t) \quad (18)$$

By (12) and (14), $z(t)/r_d = v \cos \varphi(t) - v_1(t) + c_2 r_d/c_1 \cdot \text{sat}(e(t))$ and $z(t) = 0$ yields that

$$\varphi(t) = \arccos\left(\frac{v_1(t) - q_1 \text{sat}(e(t))}{v}\right), \text{ where } q_1 = \frac{c_2 r_d}{c_1}.$$

(a) If $\varphi(t_0) \in [\arccos((q_1 + \bar{v}_o)/v), \pi - \arccos((-v_* - \bar{v}_o - q_1)/v)]$, where $0 < v_* < v - \bar{v}_o - q_1$, then $\varphi(t)$ will be also in this region for all $t \geq t_0$. To elaborate it, when $\varphi(t) = \arccos((q_1 + \bar{v}_o)/v)$, i.e., $z(t)/r_d = q_1 + q_1 \text{sat}(e(t)) + \bar{v}_o - v_1(t)$, it follows from (18) and the conditions in Proposition 2 that

$$\dot{\varphi}(t) > c_1/r_d \cdot (q_1/2) - \omega_c - 2\omega_o > 0.$$

Similarly, $\varphi(t) = \pi - \arccos((-v_* - \bar{v}_o - q_1)/v)$ leads to that $\dot{\varphi}(t) < -c_1/r_d \cdot v_* + \omega_c + \omega_o < 0$. Since $\varphi(t)$ is continuous with respect to t , the result follows.

(b) If $\varphi(t_0) \notin [\arccos((q_1 + \bar{v}_o)/v), \pi - \arccos((-v_* - \bar{v}_o - q_1)/v)]$, we show in Lemma 4 of Appendix B that there is a finite $\delta > 0$ such that $\varphi(t_0 + \delta) \in [\arccos((q_1 + \bar{v}_o)/v), \pi - \arccos((-v_* - \bar{v}_o - q_1)/v)]$.

The above implies that there exists a finite $t_1 \geq t_0$ such that $\varphi(t) \in [\arccos((q_1 + \bar{v}_o)/v), \pi - \arccos((-v_* - \bar{v}_o - q_1)/v)]$ for all $t \geq t_1$, i.e.,

$$\sin \varphi(t) \geq \sin \varphi_* = (1 - ((v_* + \bar{v}_o + q_1)/v)^2)^{1/2} \quad (19)$$

for all $t \geq t_1$.

Since v_* depends only on the control parameters in the form of c_2/c_1 , then (13) follows from (17). ■

By (13), one can easily conclude that the steady-state circumnavigating error κ is proportional to the mobility of the target, and can be made small by increasing the control parameters c_1 and c_2 . If the target is stationary, e.g., $\bar{v}_o = \bar{a}_o = 0$, then c_1 and c_2 can be selected arbitrarily large, in which case the steady-state circumnavigating error will be close to zero.

V. MOVING TARGET CIRCUMNAVIGATION UNDER THE RANGE-ONLY CONTROLLER

If the range rate $\dot{d}(t)$ is not explicitly available, we design an SOSM filter in (7) to estimate it, and use the range-only controller (9). A similar idea can also be found in [23], which only focuses on stationary target circumnavigation. Interestingly, a first-order filter and a washout filter are adopted in [29] and [30], respectively.

Proposition 3: Consider the circumnavigation system in (12) under the range-only controller in (9). If $\|\mathbf{v}_o(t)\|_2 \leq \bar{v}_o$, $\|\mathbf{a}_o(t)\|_2 \leq \bar{a}_o$, the parameters of the controller (9) and filter (7) satisfy

$$\begin{aligned} (c_1 - 1)\omega_c &> c_2 + (c_1 + 1)\omega_o, \\ c_2 &> \max((c_1 + 1)\omega_o, 2\omega_c + 4\omega_o), \\ k_1 &> 2\sigma_2, \quad k_2 > \sigma_2^2 + 2\sigma_2, \end{aligned}$$

$$\begin{aligned} k_3 &> \max(0, (k_1 + 1)\sigma_1/k_1 - k_1^2/2, \sigma_1 - 2k_1^2 - k_1^2/(2k_2)), \\ k_4 &> \max(0, k_2/2 - k_2^2, k_2^2(2k_1 + 5\sigma_1)/(k_1 - 2\sigma_2)), \end{aligned}$$

where $\sigma_1 = 2\omega_c v + c_1 \omega_c v + c_2 v + \omega_c \bar{v}_o + \bar{a}_o$ and $\sigma_2 = c_1 \omega_c$, and $d(t_0) > 2r_d + (v + \bar{v}_o)(T_1 + T_2)$, then there is a finite $T_2 > 0$ such that

$$\alpha_1(t) = d(t) \text{ and } \alpha_2(t) = \dot{d}(t), \quad \forall t > t_0 + T_2.$$

Moreover, $\limsup_{t \rightarrow \infty} |d(t) - r_d| \leq \kappa$ where κ and T_1 are given in Proposition 2.

Proof: In light of Proposition 2, we complete the proof by showing that $\alpha_1(t) = d(t)$ and $\alpha_2(t) = \dot{d}(t)$ for any $t \geq t_0 + T_2$, where T_2 is finite. Then, the circumnavigation system (12) works as exactly the case using explicit the range rate since $t_0 + T_2$. Thus, all conditions in Proposition 2 are satisfied including $d(t_0) > 2r_d + (v + \bar{v}_o)T_1$.

To this end, we define the estimating errors as

$$\xi_1(t) = d(t) - \alpha_1(t) \text{ and } \xi_2(t) = \dot{d}(t) - \alpha_2(t).$$

Then it follows from (7) and (10) that

$$\begin{aligned} \dot{\xi}_1(t) &= -k_1 |\xi_1(t)|^{1/2} \text{sgn}(\xi_1(t)) - k_2 \xi_1(t) + \xi_2(t), \\ \dot{\xi}_2(t) &= -k_3 \text{sgn}(\xi_1(t)) - k_4 \xi_1(t) + \\ &\quad v \sin \varphi(t) \left(\omega(t) - \frac{v \sin \varphi(t)}{d(t)} + \frac{v_2(t)}{d(t)} \right) + \dot{v}_1(t), \end{aligned} \quad (20)$$

where

$$\omega(t) = \omega_c + c_1/r_d \cdot (\dot{d}(t) - \xi_2(t)) + c_2 \text{sat}(e(t)).$$

Let

$$f(\xi_1, \xi_2, t) = v \sin \varphi(t) \left(\omega(t) - \frac{v \sin \varphi(t)}{d(t)} + \frac{v_2(t)}{d(t)} \right) + \dot{v}_1(t).$$

If $d(t) > r_d$, it holds that

$$|f(\xi_1(t), \xi_2(t), t)| < \sigma_1 + \sigma_2 |\xi_2(t)|, \quad (21)$$

where $\sigma_1 = 2\omega_c v + c_1 \omega_c v + c_2 v + \omega_c \bar{v}_o + \bar{a}_o$ and $\sigma_2 = c_1 \omega_c$.

Let $\boldsymbol{\xi}(t) = [|\xi_1(t)|^{1/2} \text{sgn}(\xi_1(t)), \xi_1(t), \xi_2(t)]'$ and consider the following Lyapunov function candidate

$$V_\Omega(\boldsymbol{\xi}) = \boldsymbol{\xi}' \Omega \boldsymbol{\xi},$$

where

$$\Omega = \frac{1}{2} \begin{bmatrix} 4k_4 + k_1^2 & k_1 k_2 & -k_1 \\ k_1 k_2 & 2k_4 + k_2^2 & -k_2 \\ -k_1 & -k_2 & 2 \end{bmatrix}.$$

Notice that $V_\Omega(\boldsymbol{\xi})$ is continuous but not differentiable at $\xi_1(t) = 0$, which is positive definite and radially unbounded if $k_3 > 0$ and $k_4 > 0$, i.e.,

$$\lambda_{\min}(\Omega) \|\boldsymbol{\xi}\|_2^2 \leq V_\Omega(\boldsymbol{\xi}) \leq \lambda_{\max}(\Omega) \|\boldsymbol{\xi}\|_2^2, \quad (22)$$

where $\lambda_{\min}(\Omega)$ and $\lambda_{\max}(\Omega)$ are the minimum eigenvalue and maximum eigenvalue of Ω , respectively.

Taking the derivative of $V_\Omega(\boldsymbol{\xi})$ along with (20) leads to that

$$\begin{aligned} \dot{V}_\Omega(\boldsymbol{\xi}) &= -|\xi_1(t)|^{-1/2} \boldsymbol{\xi}' Q_1 \boldsymbol{\xi} - \boldsymbol{\xi}' Q_2 \boldsymbol{\xi} + 2\xi_2(t) f(\xi_1, \xi_2, t) \\ &\quad - k_2 \xi_1(t) f(\xi_1, \xi_2, t) - k_1 |\xi_1(t)|^{1/2} \text{sgn}(\xi_1(t)) f(\xi_1, \xi_2, t), \end{aligned}$$

where

$$Q_1 = \frac{k_1}{2} \begin{bmatrix} 2k_3 + k_1^2 & 0 & -k_1 \\ 0 & 2k_4 + 5k_2^2 & -3k_1 \\ -k_1 & -3k_2 & 1 \end{bmatrix} \text{ and}$$

$$Q_2 = k_2 \begin{bmatrix} k_3 + 2k_1^2 & 0 & 0 \\ 0 & k_4 + k_2^2 & -k_2 \\ 0 & -k_2 & 1 \end{bmatrix}.$$

Together with (21), we have that

$$\begin{aligned} \text{(a)} \quad & |2\xi_2(t)f(\xi_1, \xi_2, t)| \leq 2|\xi_2(t)|(\sigma_1 + \sigma_2|\xi_2(t)|) \\ & = 2\sigma_1 \frac{1}{|\xi_1(t)|^{1/2}} \left(|\xi_1(t)|^{1/2} \text{sgn}(\xi_1(t)) |\xi_2(t)| \right) + 2\sigma_2 \xi_2^2(t) \\ & \leq \frac{\sigma_1}{|\xi_1(t)|^{1/2}} (|\xi_1(t)| + \xi_2^2(t)) + 2\sigma_2 \xi_2^2(t), \\ \text{(b)} \quad & |-k_2 \xi_1(t)f(\xi_1, \xi_2, t)| \leq k_2 |\xi_1(t)|(\sigma_1 + \sigma_2|\xi_2(t)|) \\ & \leq k_2 \sigma_1 |\xi_1(t)| + (k_2^2 \xi_1^2(t) + \sigma_2^2 \xi_2^2(t))/2, \\ \text{(c)} \quad & |-k_1 |\xi_1(t)|^{1/2} \text{sgn}(\xi_1(t)) f(\xi_1, \xi_2, t)| \\ & \leq |k_1 |\xi_1(t)|^{-1/2} \text{sgn}(\xi_1(t))|(\sigma_1 + \sigma_2|\xi_2(t)|) \\ & \leq k_1 \sigma_1 |\xi_1(t)|^{-1/2} |\xi_1(t)|^2 + (k_1^2 |\xi_1(t)| + \sigma_2^2 \xi_2^2(t))/2. \end{aligned}$$

Then, it holds that

$$\dot{V}_\Omega(\xi) \leq -|\xi_1(t)|^{-1/2} \xi'(Q_1 - Q_3)\xi - \xi'(Q_2 - Q_4)\xi,$$

where

$$Q_3 = \begin{bmatrix} (k_1 + 1)\sigma_1 & 0 & 0 \\ 0 & 0 & 0 \\ 0 & 0 & \sigma_1 \end{bmatrix} \text{ and}$$

$$Q_4 = \begin{bmatrix} k_2 \sigma_1 + k_1^2/2 & 0 & 0 \\ 0 & k_2^2/2 & 0 \\ 0 & 0 & 2\sigma_2 + \sigma_2^2 \end{bmatrix}.$$

If $k_1 > 2\sigma_1$, $k_2 > 0$, $k_3 > \max(0, (k_1 + 1)\sigma_1/k_1 - k_1^2/2)$, and $k_4 > k_2^2(2k_1 + 5\sigma_1)/(k_1 - 2\sigma_2)$, then $Q_1 - Q_3$ is positive definite. Similarly, the conditions $k_1 > 0$, $k_2 > \sigma_2^2 + 2\sigma_2$, $k_3 > \max(0, \sigma_1 - 2k_1^2 - k_1^2/(2k_2))$ and $k_4 > \max(0, k_2/2 - k_2^2)$ lead to that $Q_2 - Q_4$ is positive definite.

Overall, the conditions on controller and filter parameters ensure that

$$\begin{aligned} \dot{V}_\Omega(\xi) & \leq -|\xi_1(t)|^{-1/2} \xi'(Q_1 - Q_3)\xi \\ & \leq -|\xi_1(t)|^{-1/2} \lambda_{\min}(Q_1 - Q_3) \|\xi\|_2^2. \end{aligned} \quad (23)$$

It follows from (22), (23), and the fact

$$|\xi_1(t)|^{1/2} \leq \|\xi\|_2 \leq V_\Omega^{1/2}(\xi)/\lambda_{\min}^{1/2}(\Omega)$$

that

$$\dot{V}_\Omega(\xi) \leq -\frac{\lambda_{\min}^{1/2}(\Omega)}{V_\Omega^{1/2}(\xi)} \lambda_{\min}(Q_1 - Q_3) \|\xi\|_2^2 \leq -\gamma V_\Omega^{1/2}(\xi),$$

where $\gamma = \frac{\lambda_{\min}^{1/2}(\Omega) \lambda_{\min}(Q_1 - Q_3)}{\lambda_{\max}(\Omega)}$. By the comparison principle [35], we finally have that

$$\alpha_1(t) = d(t) \text{ and } \alpha_2(t) = \dot{d}(t), \quad \forall t > t_0 + T_2,$$

where $T_2 = 2V_\Omega^{1/2}(\xi(t_0))/\gamma^2$. This implies that the controller (9) is exactly identical to that in (6) for all $t > t_0 + T_2$ if

²We can set $\alpha_1(t_0) = d(t_0)$ to reduce the convergence time T_2 in the implementation.

TABLE II
PARAMETERS OF THE RANGE-BASED CONTROLLER (6)

Parameter	c_1	c_2
Value	200	30

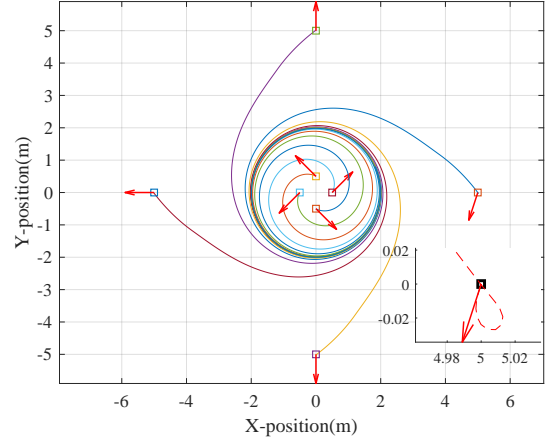


Fig. 2. Trajectories of the pursuer with different initial states.

$d(t_0 + T_2) > 2r_d + (v + \bar{v}_o)T_1$. The rest of the proof follow from that of Proposition 2. ■

VI. SIMULATIONS

For brevity, we denote $s_o(t) = [p_o'(t), v_o(t)]'$ and $s(t) = [p'(t), \theta(t)]'$ denote the states of the target and pursuer. The linear speed of the pursuer is set as $v = 0.5$ m/s. Note that simulations in Sections VI-A, VI-B and VI-C are performed under the range-based controller (6), while Section VI-D and VI-E are under the range-only controller (9). Furthermore, we adopt a 6-DOF fixed-wing UAV and take the noisy measurements into account in Section VI-E.

A. Stationary target circumnavigation

Let $p_o(t_0) = [0, 0]'$. To test the global stability of the proposed controller, we set eight different initial states for the pursuer, i.e., $s(t_0) = [5, 0, -0.6\pi]$, $[0, 5, 0.5\pi]$, $[-5, 0, \pi]$, $[0, -5, -0.5\pi]$, $[0.5, 0, 0.25\pi]$, $[0, 0.5, 0.75\pi]$, $[-0.5, 0, -0.75\pi]$, and $[0, -0.5, -0.25\pi]$, see Fig. 2. The square and the arrow denote the initial position and course, respectively. All trajectories of the pursuer form a circle centered at the target with the radius $r_d = 2$ m, under the range-based controller (6) with the parameters in Table II.

Taking the trajectory starting at $s(t_0) = [5, 0, -0.6\pi]$ as an example, the distance $d(t)$ and angle $\varphi(t)$ versus time are shown in Fig. 3. The dash lines represent the desired radius $r_d = 2$ and reference angle $\pi/2$, respectively. It is clear that the target circumnavigation task is eventually completed in the sense of (3).

B. Moving target circumnavigation

Let $s_o(t_0) = [0, 0, -\sqrt{2}\bar{v}_o/2, -\sqrt{2}\bar{v}_o/2]'$, $s(t_0) = [5, 0, -0.6\pi]'$, where $\bar{v}_o = 0.15$. Moreover, the acceleration $a_o(t)$ of the target is generated by a uniform distribution, i.e.,

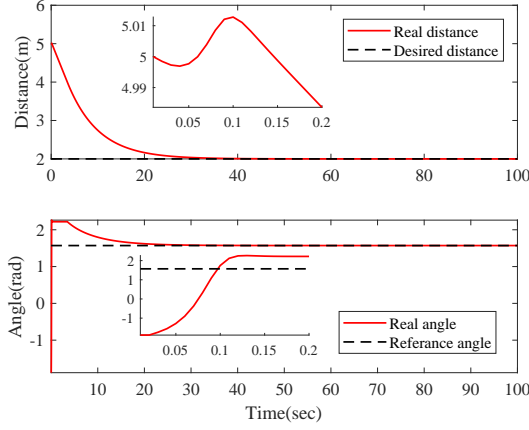


Fig. 3. Distance $d(t)$ and angle $\varphi(t)$ versus time when the target is stationary.

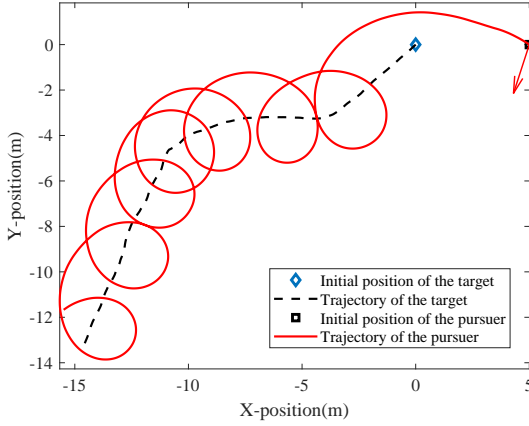


Fig. 4. Trajectories of the target and pursuer.

$\mathbf{a}_o(t) \sim \sqrt{2}\bar{a}_o \times \mathcal{U}(-0.5, 0.5)$, where $\bar{a}_o = 0.2$. The control parameters are selected as those in Table II. In this case, Fig. 4 shows the trajectories of the target and pursuer, where the arrow denotes the initial course of the pursuer. Moreover, it can be observed from Fig. 5 that $\varphi(t)$ is trapped in a vicinity of $\pi/2$, moreover, both $|d(t) - r_d|$ and $|z(t)|$ are bounded by a small constant, as $t \rightarrow \infty$. This validates the results of Proposition 2.

C. Comparison with the existing methods

For comparison, we consider the constraint on control input and let $|\omega(t)| \leq \bar{\omega}$, where $\bar{\omega} = 1$ rad/s [2] in this subsection. The comparison methods are the geometrical approach [23] with parameters $k = 1$ and $r_a = 9.95$, the switching approach [24] with parameter $k = 1.4/r_d$, the sliding mode approach [2] with $\delta = 0.83$ and $\gamma = 0.3$ and the backstepping approach [34] with $k_1 = 20$ and $k_2 = 0.3$.

When the target is stationary, the performance comparison is depicted in Fig. 6, wherein $\mathbf{s}(t_0) = [3, 3, -0.75\pi]'$. One can easily observe that all methods other than the sliding mode approach can complete the task with zero steady-state error. However, both the geometrical approach and the switching approach have large overshoot.

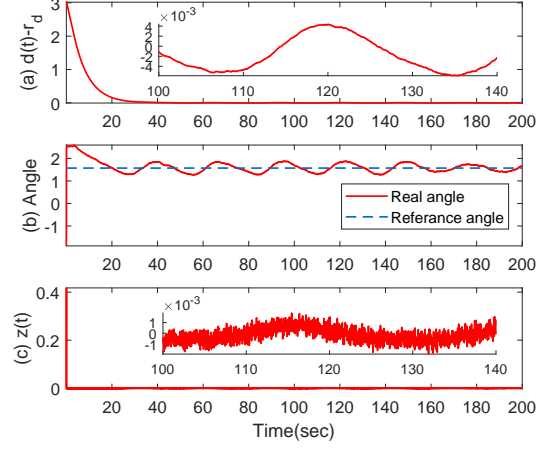


Fig. 5. Results versus time with a moving target: (a) circumnavigating error $d(t) - r_d$; (b) angle $\varphi(t)$ and reference angle $\pi/2$; (c) error $z(t) = \dot{e}(t) + c_2/c_1 \cdot e(t)$.

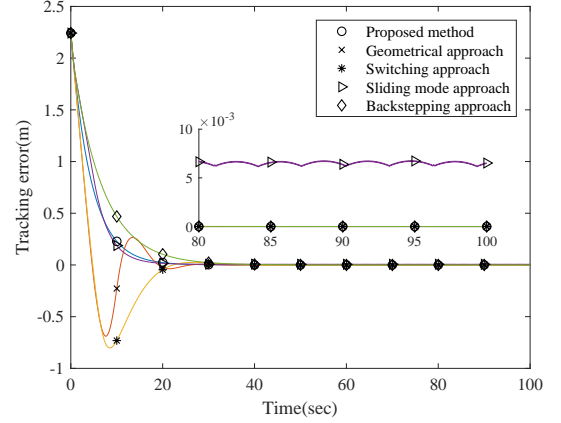


Fig. 6. Performance comparison when the target is stationary.

If the target is moving as described in Section VI-B, Fig. 7 illustrates the results with $\mathbf{s}_o(t_0) = [0, 0, -\sqrt{2}\bar{v}_o/2, -\sqrt{2}\bar{v}_o/2]'$ and $\mathbf{s}(t_0) = [5, 0, -0.6\pi]'$. Since both the geometrical approach and the switching approach are designed for the stationary target, they cannot solve the case of a moving target. The performance of our controller is similar to that of the sliding mode approach. However, the mean-square steady-state circumnavigating error (MSSE)³ of our controller is 0.015 while that of the sliding mode approach is 0.101, in the time interval from 160 s to 200 s, see the partially enlarged view of Fig. 7. Moreover, Fig. 8 also illustrates that the range-based controller (6) is more energy efficient than the sliding mode approach.

Overall, the range-based controller in (6) outperforms the methods in [2], [23], [24]. Particularly, our method is effective in handling the problem of moving target circumnavigation.

D. Target Circumnavigation with Estimated Range Rate

In this subsection, we evaluate the controller (9) with the estimated range rate $\alpha_2(t)$ of the SOSM filter (7). The

³MSSE = $\frac{1}{n} \sum_{i=1}^n (d(i) - r_d)^2$ where i denotes the i -th time step.

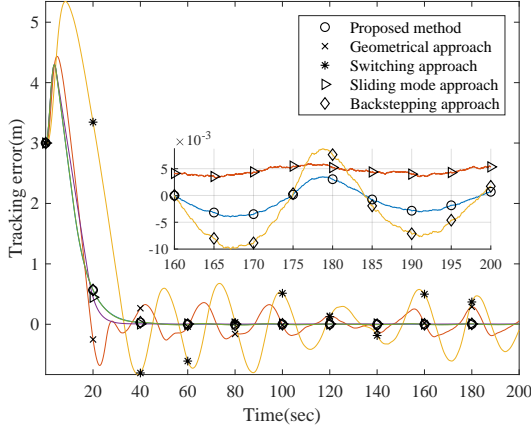


Fig. 7. Performance comparison when the target is moving.

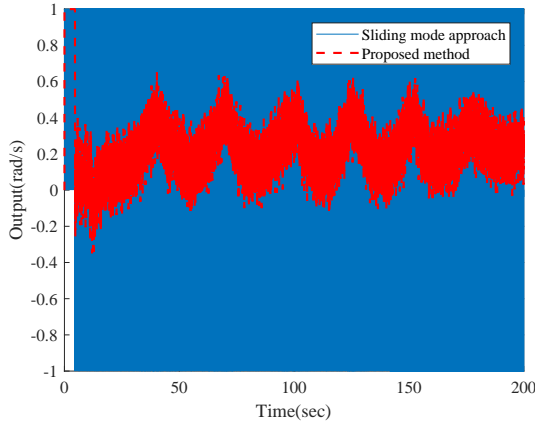


Fig. 8. Outputs of the sliding mode approach and our range-based controller when the target is moving.

TABLE III
PARAMETERS OF THE RANGE-ONLY CONTROLLER (9) AND FILTER (7)

Parameter	c_1	c_2	k_1	k_2	k_3	k_4
Value	8	1	4	8	0.01	200

parameters are selected as those in Table III, satisfying all conditions in Proposition 3. Fig. 9 and Fig. 10 show the trajectory of the pursuer with a desired radius $r_d = 2$, the estimated range rate $\alpha_2(t)$ and actual range rate $\dot{d}(t)$. It can be observed that $\alpha_2(t)$ approaches $\dot{d}(t)$ in finite time.

E. Target Circumnavigation by a Fixed-wing UAV

Finally, a 6-DOF fixed-wing UAV is adopted to test the effectiveness of the range-only controller (9), see Fig. 11. To be consistent with the notions in [9], [37], we also apply $[p_n, p_e, p_d]'$ and $[\phi, \theta, \psi]'$ to denote the position and orientation of the UAV in the inertial coordinate frame, respectively. Moreover, we use $[u, v, w]'$ and $[p, q, r]'$ to denote the linear velocities and angular rates in the body frame. Due to the page limitation, we omit details of the complicated mathematical model of the UAV, which can be found in [37], and adopt codes from [38] for the model. Trajectories of the target and the UAV are shown in Fig. 12, where the circle and square

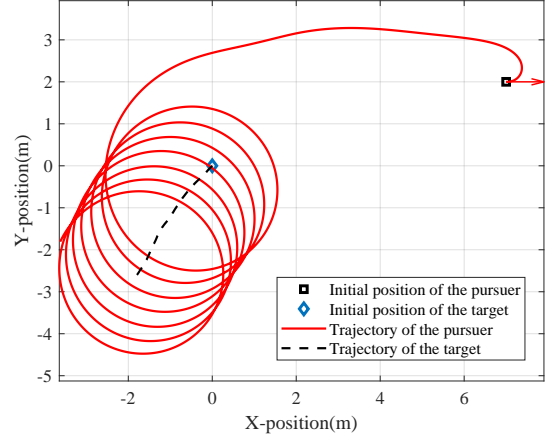


Fig. 9. Performance of the controller (9) with estimated range rate $\alpha_2(t)$.

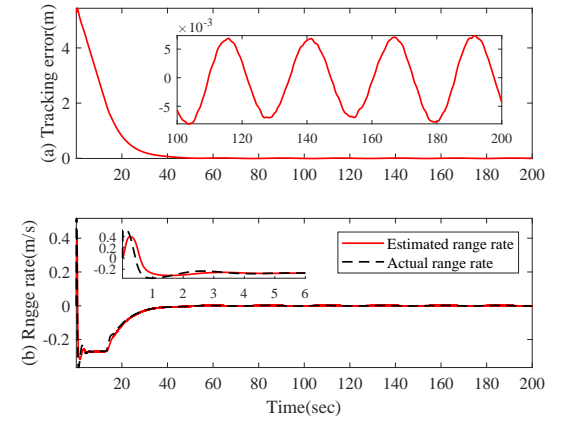


Fig. 10. Simulation results: (a) circumnavigating error of the SOSM filter; (b) estimated range rate $\alpha_2(t)$ and actual range rate $\dot{d}(t)$.

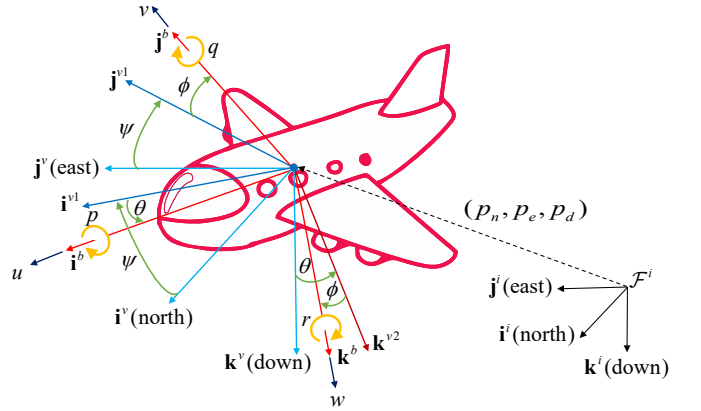


Fig. 11. A fixed-wing UAV in [9].

denote their initial positions and the desired radius is set as 400 m. Furthermore, the circumnavigating error is illustrated by Fig. 13(a). The actual range rate and its estimated version are depicted by Fig. 13(b), respectively. Note that the desired altitude and forward speed of the UAV are set as -100 m and 30 m/s, which are possessed by the controllers in [38].

Then, consider the situation that range measurements are

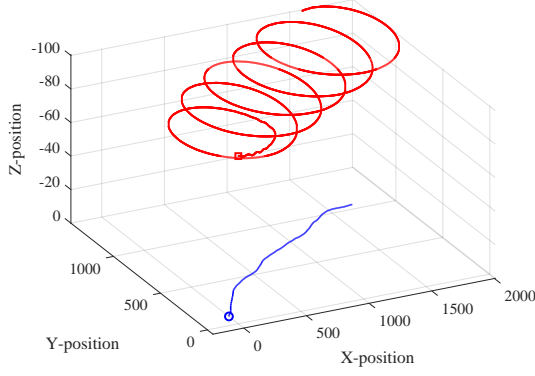


Fig. 12. 3D trajectories of the target and fixed-wing UAV.

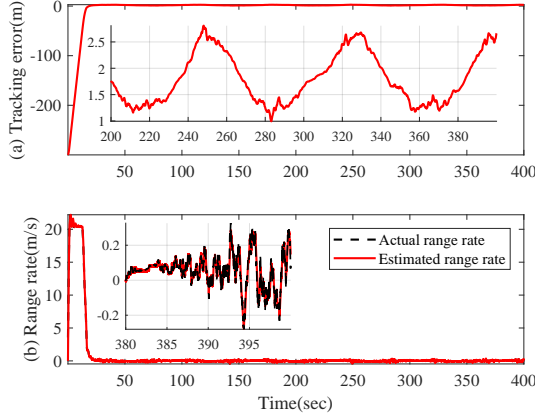


Fig. 13. Simulation results: (a) circumnavigating error; (b) actual range rate and its estimated version.

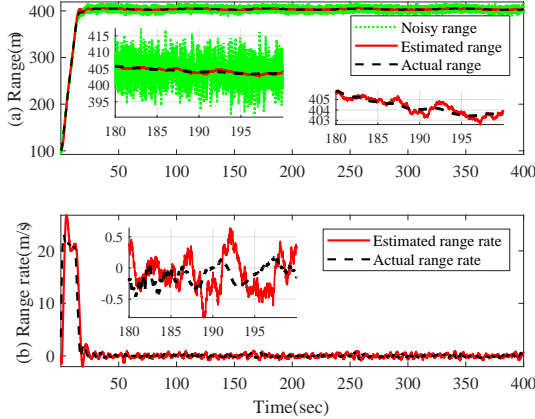


Fig. 14. Range and range rate versus time with measurement noises.

corrupted by an additive Gaussian noise, i.e.,

$$d(t) = \|\mathbf{p}(t) - \mathbf{p}_o(t)\|_2 + w(t),$$

where $w(t) \sim \mathcal{N}(0, \sigma^2)$. The range and range rate versus time are depicted by Fig. 14 with $r_d = 400$ and $\sigma = 4$. One can observe that the maximum circumnavigating error (dash line in Fig. 14) is not larger than 6 m, which implies that the performance of the proposed controller is not significantly degraded.

VII. CONCLUSION

In this paper, we have proposed a range-only controller to drive an underactuated pursuer to circumnavigate a fully actuated target with a predefined radius. Given that both the range and range rate measurements are known, the proposed controller has a simple PD-like form with a bias to eliminate steady-state circumnavigating error. Thus, for a stationary target, the controller can ensure global convergence and local exponential stability near the equilibrium with zero steady-state error. Moreover, we explicitly showed that the upper bound of the circumnavigating error is proportional to the maximum linear speed and acceleration of the target. Furthermore, we revised the range-based controller by replacing the actual range rate with its estimated version by designing an SOSM filter. Finally, the simulations validated our theoretical results.

APPENDIX

A. Proof of Proposition 1

To prove Proposition 1, we first show that there exists a finite time instant $t_1 \geq t_0$ such that $\varphi(t) \in [0, \pi], \forall t \geq t_1$ for any initial state, see Lemma 1. Then, the closed-loop system in (10) under (6) is shown to be asymptotically stable with an exponential convergence speed.

Lemma 1: Under the conditions in Proposition 1, there exists a finite time instant $t_1 \geq t_0$ such that $\varphi(t) \in [0, \pi], \forall t \geq t_1$, for any initial state $\varphi(t_0) \in (-\pi, \pi]$.

Proof: Inserting (9) to (10) yields that

$$\dot{\varphi}(t) = \omega_c + \frac{c_1}{r_d} \dot{d}(t) + c_2 \text{sat} \left(\frac{d(t) - r_d}{r_d} \right) - \frac{v \sin \varphi(t)}{d(t)}. \quad (24)$$

If $\varphi(t) = 0$, it follows from (24) that

$$\dot{\varphi}(t) \geq (1 + c_1)\omega_c - c_2 > 0. \quad (25)$$

Similarly, $\varphi(t) = \pi$ leads to that

$$\dot{\varphi}(t) \leq (1 - c_1)\omega_c + c_2 < 0. \quad (26)$$

Together with the fact that $\dot{\varphi}(t)$ is continuous with respect to t , it implies that $\varphi(t) \in [0, \pi]$ for all $t \geq t_0$ if $\varphi(t_0) \in [0, \pi]$.

Next, we only need to show that there exists a finite time instant $t_1 > t_0$ such that $\varphi(t_1) \in [0, \pi]$ if $\varphi(t_0) \in (-\pi, 0)$. To this end, four cases in Fig. 15 are considered.

For the case in Fig. 15(a), i.e., $d(t_0) \in [r_d, \infty)$ and $\varphi(t_0) \in [-\pi/2, 0)$, it follows from (10) and (24) that $\dot{d}(t_0) \geq 0$ and $\dot{\varphi}(t_0) > \omega_c$. Since $\dot{\varphi}(t)$ is continuous with respect to t , there exists a $\delta > 0$ such that $\varphi(t_0 + \delta) > -\pi/2 + \delta\omega_c \geq 0$.

For the case in Fig. 15(b), i.e., $d(t_0) \in [r_d, \infty)$ and $\varphi(t_0) \in (-\pi, -\pi/2)$, it follows from (24) and (26) that

$$\begin{cases} \dot{\varphi}(t) > 0, & \text{if } \varphi(t) = -\pi/2, \\ \dot{\varphi}(t) < 0, & \text{if } \varphi(t) = -\pi. \end{cases}$$

Thus, there are three possible results after some finite time $\delta > 0$: (i) $\varphi(t_0 + \delta) \leq -\pi$ and $d(t_0 + \delta) \geq r_d$, which is equivalent to that $\varphi(t_0 + \delta) \geq 0$; (ii) $\varphi(t_0 + \delta) \geq -\pi/2$ and $d(t_0 + \delta) \geq r_d$, which is the case shown in Fig. 15(a); (iii) $d(t_0 + \delta) < r_d$, which is to be shown in Fig. 15(c) and Fig. 15(d).

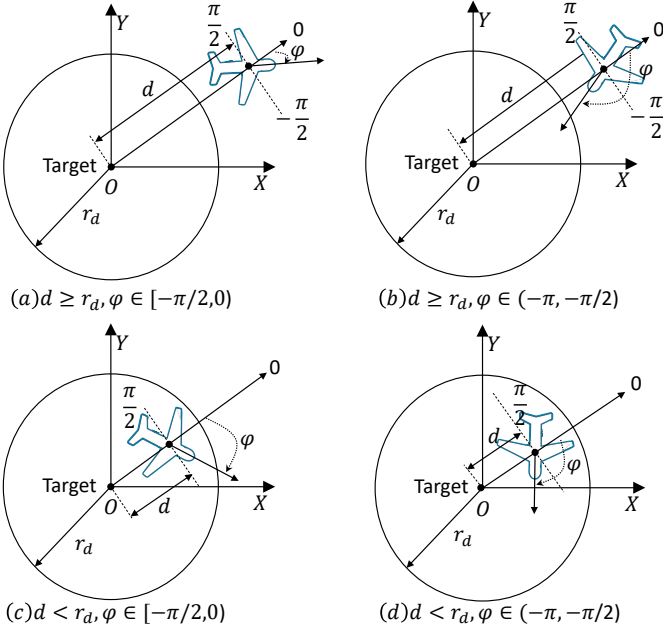


Fig. 15. Illustrations of the pursuer state.

When $\varphi(t) = -\pi/2$ and $d(t) > 0$, it follows from (24) that

$$\dot{\varphi}(t) = \frac{c_2}{r_d d(t)} \left(d^2(t) + \frac{v - c_2 r_d}{c_2} d(t) + \frac{v r_d}{c_2} \right). \quad (27)$$

- (a) If $c_2 < (3 + 2\sqrt{2})\omega_c$, then (27) yields that $\dot{\varphi}(t) > 0$.
- (b) If $c_2 \geq (3 + 2\sqrt{2})\omega_c$, there may exist $x_0 = [d_*, -\pi/2]'$ such that $\dot{\varphi}(t) = 0$, where $d_* \in (0, r_d)$. However, the equilibrium x_0 is unstable and there is no closed orbit around it. The verification will be shown later.

Overall, there are only two possibilities after some finite $\delta > 0$: (i) $d(t_0 + \delta) \geq r_d$ and $\varphi(t_0 + \delta) \in [-\pi/2, 0)$, which is Fig. 15(a); (ii) $\varphi(t_0 + \delta) \in [0, \pi]$. Then, we conclude that there exists a finite time instant t_1 such that $\varphi(t_1) \in [0, \pi]$ for any initial $\varphi(t_0) \in (-\pi, 0)$.

To prove (b), we linearize the system in (10) around x_0 as follows

$$\dot{x}(t) = A(x(t) - x_0),$$

where the Jacobian matrix A is directly obtained as

$$A = \begin{bmatrix} 0 & v \\ c_2/r_d - v/d_*^2 & c_1\omega_c \end{bmatrix}.$$

It is clear that matrix A at least has one unstable eigenvalue. To be more specific, (i) when $c_2 = (3 + 2\sqrt{2})\omega_c$, the unique equilibrium is $x_0 = [r_d/2 - v/(2c_2), -\pi/2]'$, and the other eigenvalue of A is zero; (ii) $c_2 > (3 + 2\sqrt{2})\omega_c$, the equilibrium point lying in $(r_d/2 - v/(2c_2), r_d)$ is a saddle, and the other is an unstable node or focus. In any case of (i) and (ii), all trajectories starting near x_0 will diverge away from it in finite time [35]. However, this is only local performance and it is not sufficient to conclude that there are no closed orbits around the equilibrium lying in $(0, r_d/2 - v/(2c_2))$ by Lemma 2.1 (Poincaré-Bendixson Criterion) and Corollary 2.1 of [35]. To rule out this case, we apply the Dulac's Criterion

of [39, Section 7.2] by selecting a continuously differentiable, real-value function $g(x) = x_1(t)$. When $x_1(t) \in (0, r_d)$ and $x_2(t) \in (-\pi, 0)$, it holds that

$$\frac{\partial(g(x)\dot{x}_1)}{\partial x_1} + \frac{\partial(g(x)\dot{x}_2)}{\partial x_2} = -c_1\omega_c x_1(t) \sin x_2(t) > 0.$$

Thus, there is no closed orbit when the pursuer travels in the region $x_1(t) \in (0, r_d)$ and $x_2(t) \in (-\pi, 0)$. ■

Lemma 2: Under the conditions in Proposition 1, the closed-loop system in (10) is asymptotically stable.

Proof: By Lemma 1, there exists a finite t_1 such that $x_2(t) \in [0, \pi]$, $\forall t \geq t_1$.

Consider a Lyapunov function candidate [24] as

$$V(x) = \int_{r_d}^{x_1(t)} c_2 \text{sat}\left(\frac{\tau - r_d}{r_d}\right) d\tau + \int_{r_d}^{x_1(t)} \left(\frac{1}{r_d} - \frac{1}{\tau}\right) d\tau + 1 - \sin x_2(t).$$

Taking the time derivative of $V(x)$ along with (10) leads to that

$$\begin{aligned} \dot{V}(x) &= c_2 \text{sat}(e(t)) \dot{x}_1(t) - \left(\omega(t) - \frac{v \sin x_2(t)}{x_1(t)} \right) \cos x_2(t) \\ &= -v \cos x_2(t) \times \\ &\quad \left(\frac{v}{x_1(t)} - \frac{v}{x_1(t)} \sin x_2(t) + c_1\omega_c \cos x_2(t) \right). \end{aligned} \quad (28)$$

- (a) If $x_2(t) \in [0, \pi/2]$, we have that $\cos x_2(t) \geq 0$, and $1 - \sin x_2(t) \geq 0$. It follows from (28) that

$$\dot{V}(x) \leq 0.$$

- (b) If $x_2(t) \in (\pi/2, \pi]$, then $\cos x_2(t) < 0$. To determine the sign of $\dot{V}(x)$, three cases are considered as follows.

- (i) For $x_1(t) \geq r_d$, we have that

$$c_1\omega_c \cos x_2(t) < \omega_c \cos x_2(t) \leq v/x_1(t) \cdot \cos x_2(t),$$

where the inequality uses the fact $c_1 > 1$ in (11). Consequently, it follows from (28) that $\dot{V}(x) < 0$.

- (ii) For $v/(c_1\omega_c) < x_1(t) < r_d$, it holds that

$$x_1(t) > -\frac{v}{c_1\omega_c} \frac{1 - \sin x_2}{\cos x_2},$$

which yields that

$$\frac{v}{x_1(t)} - \frac{v}{x_1(t)} \sin x_2(t) + c_1\omega_c \cos x_2(t) < 0.$$

Jointly with (28), it can be easily verified that $\dot{V}(x) < 0$.

- (iii) For $0 < x_1(t) \leq v/(c_1\omega_c)$, it follows from (24) that

$$\begin{aligned} \dot{x}_2(t) &\leq \omega_c + \frac{c_2}{r_d} (d(t) - r_d) + c_1\omega_c (\cos \varphi(t) - \sin \varphi(t)) \\ &< \omega_c - c_1\omega_c + c_2/r_d \cdot (d(t) - r_d) \\ &< \omega_c - c_1\omega_c < 0. \end{aligned}$$

This implies that $x_2(t)$ will enter the region $[0, \pi/2]$ in some finite time. When $x_2(t) = \pi/2$, it holds that

$$\begin{cases} \dot{x}_2(t) > 0, & \text{if } x_1(t) \in (0, r_d), \\ \dot{x}_2(t) = 0, & \text{if } x_1(t) = r_d, \\ \dot{x}_2(t) < 0, & \text{if } x_1(t) \in (r_d, \infty). \end{cases}$$

Thus, the pursuer states never return to $0 < x_1(t) \leq v/c_1\omega_c$ and $\pi/2 < x_2 \leq \pi$. Finally, we have $\dot{V}(\mathbf{x}) \leq 0$ by case (a).

However, $\dot{V}(\mathbf{x})$ is not negative definite, since $\dot{V}(\mathbf{x}) = 0$ for $x_2(t) = \pi/2$ and any $x_1(t)$. Let $\mathcal{S} = \{\mathbf{x} | \dot{V}(\mathbf{x}) = 0\}$, and suppose that $\tilde{\mathbf{x}}_e$ is an element of \mathcal{S} except \mathbf{x}_e . Then

$$\dot{x}_2|_{\mathbf{x}=\tilde{\mathbf{x}}_e} = \omega_c - v/x_1(t) + c_2 \text{sat}(e(t)) \neq 0.$$

So, no solution can stay identically in \mathcal{S} other than the trivial solution $\mathbf{x}(t) \equiv \mathbf{x}_e$.

Moreover, $V(\mathbf{x})$ is nonnegative, and $V(\mathbf{x}) > 0, \forall \mathbf{x} \neq \mathbf{x}_e$. By the LaSalle's invariance theorem [35, Corollary 4.1], \mathbf{x}_e is an asymptotically stable equilibrium of the closed-loop system in (10) under the range-based controller (6). ■

If a closed-loop system is locally exponentially stable near the equilibrium, then this system is robust against perturbations [24], [35]. Lemma 3 further shows that the range-based controller in (6) can ensure that \mathbf{x}_e is an exponentially stable equilibrium.

Lemma 3: Under the conditions in Proposition 1, there exists a finite $t_1 \geq t_0$ such that

$$\|\mathbf{x}(t) - \mathbf{x}_e\| \leq C\|\mathbf{x}(t_1) - \mathbf{x}_e\| \exp(-\rho(t - t_1)), \forall t > t_1,$$

where ρ and C are two positive constants.

Proof: By Lemma 2, the closed-loop system (10) has a globally stable equilibrium \mathbf{x}_e . Thus, the closed-loop system in (10) near this equilibrium can be written as

$$\begin{aligned} \dot{x}_1(t) &= v \cos x_2(t), \\ \dot{x}_2(t) &= \omega_c + c_1\omega_c \cos x_2(t) + c_2/r_d \cdot (x_1(t) - r_d) \\ &\quad - (v \sin x_2(t))/x_1(t). \end{aligned} \quad (29)$$

Then, the linearization around \mathbf{x}_e is directly obtained from (29) that

$$\dot{\mathbf{x}}(t) = F(\mathbf{x}(t) - \mathbf{x}_e), \quad (30)$$

where the Jacobian matrix F is given as

$$F = \begin{bmatrix} 0 & -v \\ c_2/r_d + \omega_c/r_d & -c_1\omega_c \end{bmatrix}.$$

Obviously, both the eigenvalues of F have negative real part, i.e., F is Hurwitz.

Let $\mathcal{D} = \{\mathbf{x} | V(\mathbf{x}) \leq b\}$, where $b > 0$. If b is sufficiently small, then $d(t)$ is sufficiently close to r_d and $\varphi(t)$ is sufficiently close to $\pi/2$. Furthermore, the closed-loop system in (29) is continuously differentiable in \mathcal{D} . By [35, Corollary 4.3], \mathbf{x}_e is an exponentially stable equilibrium for the closed-loop system in (10).

Thus, there exists a finite t_1 such that $\mathbf{x}(t) \in \mathcal{D}$ for all $t > t_1$. And it follows from (30) that the trajectory of this system satisfies that

$$\mathbf{x}(t) - \mathbf{x}_e = Q \exp(\Lambda(t - t_1))Q^{-1}(\mathbf{x}(t_1) - \mathbf{x}_e), \forall t > t_1,$$

where $F = Q\Lambda Q^{-1}$, $\Lambda = \text{diag}(\lambda_1, \lambda_2)$, and $\lambda_i, i = 1, 2$ are the eigenvalues of matrix F . Finally, it holds that

$$\begin{aligned} \|\mathbf{x}(t) - \mathbf{x}_e\| &= \|Q \exp(\Lambda(t - t_1))Q^{-1}(\mathbf{x}(t_1) - \mathbf{x}_e)\| \\ &\leq C\|\mathbf{x}(t_1) - \mathbf{x}_e\| \exp(-\rho(t - t_1)), \end{aligned}$$

where $C = \|Q\|\|Q^{-1}\|$, $\Delta = (c_1\omega_c)^2 - 4(c_2\omega_c + \omega_c^2)$, and

$$\rho = \begin{cases} (c_1\omega_c - \sqrt{\Delta})/2, & \text{if } \Delta > 0, \\ c_1\omega_c/2, & \text{if } \Delta \leq 0. \end{cases}$$

■

Proof of Proposition 1. In Lemma 1, it has been proved that there exists a finite time instant $t_1 \geq t_0$ such that $\varphi(t) \in [0, \pi], \forall t \geq t_1$, for any initial state $\varphi(t_0) \in (-\pi, \pi]$. Then, the closed-loop system in (10) asymptotically converges to the equilibrium \mathbf{x}_e in light of Lemma 2. Furthermore, \mathbf{x}_e is an exponentially stable equilibrium by Lemma 3.

B. Proof of Proposition 2

Lemma 4: Under the conditions in Proposition 2, there is a finite $t_1 \geq t_0$ such that $\varphi(t_1) \in [\arccos((q_1 + \bar{v}_o)/v), \pi - \arccos(-v_* - \bar{v}_o - q_1)/v]$ and $d(t_1) > 2r_d$, where $q_1 = c_2r_d/c_1$.

Proof: If $\varphi(t_0) \in [\arccos((q_1 + \bar{v}_o)/v), \pi - \arccos(-v_* - \bar{v}_o - q_1)/v]$, the proof is finished. Thus, we only need to analyze the case that $\varphi(t_0)$ does not belong to the foregoing region.

When $d(t) \geq 2r_d$, it follows from (18) that

$$\begin{aligned} \dot{\varphi}(t) &= c_1/r_d \cdot (v \cos \varphi(t) - v_1(t) + q_1) \\ &\quad + v/r_d - v \sin \varphi(t)/d(t) + v_2(t)/d(t). \end{aligned} \quad (31)$$

(i) If $\varphi(t) \in (-\arccos((\bar{v}_o - q_1)/v), \arccos((q_1 + \bar{v}_o)/v))$, then (31) leads to that

$$\dot{\varphi}(t) > (v - \bar{v}_o)/2r_d + c_1/r_d \cdot (\bar{v}_o - v_1(t)) > 0.$$

(ii) If $\varphi(t) \in (\pi - \arccos((-v_* - \bar{v}_o - q_1)/v), \pi] \cap (-\pi, -\pi + \arccos((-v_* - \bar{v}_o - q_1)/v)]$, where $0 < v_* < v - \bar{v}_o - q_1$, then it follows from (18) and the conditions in Proposition 2 that

$$\dot{\varphi}(t) < -c_1/r_d \cdot v_* + \omega_c + \omega_o < 0. \quad (32)$$

Moreover, the maximum time for $\varphi(t)$ to pass through $\pi - \arccos((-v_* - \bar{v}_o - q_1)/v)$ is given as

$$T_3 = \frac{2 \arccos((-v_* - \bar{v}_o - q_1)/v)}{c_1/r_d \cdot v_* - \omega_c - \omega_o}.$$

(iii) If $\varphi(t) \in (-\pi + \arccos((-v_* - \bar{v}_o - q_1)/v), -\arccos((\bar{v}_o - q_1)/v))$, then $\varphi(t)$ either enters case (i) or case (ii) in a finite time, by (15) and Lemma 6.1 of [2]. That is

$$T_4 = \max \left(\frac{\pi}{c_1/r_d \cdot v_* - \omega_c - \omega_o}, \frac{\pi}{c_2 - c_1\omega_o} \right).$$

The analysis is of the same as that of Lemma 1 and is omitted.

Thus, there is a finite $t_1 \geq t_0$ such that $\varphi(t_1) \in [\arccos((\bar{v}_o + q_1)/v), \pi - \arccos((-v_* - \bar{v}_o - q_1)/v)]$.

Furthermore, we consider the variation of $d(t)$ meanwhile $\varphi(t)$ enters the desired region. Case (i) implies that $\dot{d}(t) > 0$ by (12). Hence, only cases (ii) and (iii) may result in the decrease of $d(t)$. Therefore, it holds that $d(t_1) > 2r_d$ by $d(t_0) > 2r_d + (v + \bar{v}_o)T_1$ where $T_1 = T_3 + T_4$. ■

REFERENCES

- [1] I. Shames, S. Dasgupta, B. Fidan, and B. D. O. Anderson, "Circumnavigation using distance measurements under slow drift," *IEEE Transactions on Automatic Control*, vol. 57, no. 4, pp. 889–903, 2012.
- [2] A. S. Matveev, H. Teimoori, and A. V. Savkin, "Range-only measurements based target following for wheeled mobile robots," *Automatica*, vol. 47, no. 1, pp. 177–184, 2011.
- [3] V. N. Dobrokhodov, I. I. Kaminer, K. D. Jones, and R. Ghabcheloo, "Vision-based tracking and motion estimation for moving targets using unmanned air vehicles," *Journal of Guidance Control & Dynamics*, vol. 31, no. 4, pp. 907–917, 2008.
- [4] P. B. Sujit, S. Saripalli, and J. B. Sousa, "Unmanned aerial vehicle path following: A survey and analysis of algorithms for fixed-wing unmanned aerial vehicles," *IEEE Control Systems*, vol. 34, no. 1, pp. 42–59, 2014.
- [5] A. S. Matveev, H. Teimoori, and A. V. Savkin, "Navigation of a unicycle-like mobile robot for environmental extremum seeking," *Automatica*, vol. 47, no. 1, pp. 85–91, 2011.
- [6] K. Ovchinnikov, A. Semakova, and A. Matveev, "Cooperative surveillance of unknown environmental boundaries by multiple nonholonomic robots," *Robotics & Autonomous Systems*, vol. 72, pp. 164–180, 2015.
- [7] D. Lawrence, "Lyapunov vector fields for UAV flock coordination," in *2nd AIAA Unmanned Unlimited Conference, Workshop, and Exhibit*, 2003.
- [8] E. W. Frew, D. A. Lawrence, and M. Steve, "Coordinated standoff tracking of moving targets using Lyapunov guidance vector fields," *Journal of Guidance Control & Dynamics*, vol. 31, no. 2, pp. 290–306, 2008.
- [9] F. Dong, K. You, and J. Zhang, "Flight control for UAV loitering over a ground target with unknown maneuver," *IEEE Transactions on Control Systems Technology*, 2019.
- [10] M. Michaek and K. Kozowski, "Vector-field-orientation feedback control method for a differentially driven vehicle," *IEEE Transactions on Control Systems Technology*, vol. 18, no. 1, pp. 45–65, 2010.
- [11] R. W. Beard, J. Ferrin, and J. Humpherys, "Fixed wing UAV path following in wind with input constraints," *IEEE Transactions on Control Systems Technology*, vol. 22, no. 6, pp. 2103–2117, 2014.
- [12] Y. A. Kapitanuk, A. V. Proskurnikov, and M. Cao, "A guiding vector-field algorithm for path-following control of nonholonomic mobile robots," *IEEE Transactions on Control Systems Technology*, vol. 26, no. 4, pp. 1372–1385, 2018.
- [13] K. Cao, Z. Qiu, and L. Xie, "Relative docking and formation control via range and odometry measurements," *IEEE Transactions on Control of Network Systems*, 2019.
- [14] P. Li, G. Pin, G. Fedele, and T. Parisini, "Deadbeat source localization from range-only measurements: A robust kernel-based approach," *IEEE Transactions on Control Systems Technology*, vol. 27, no. 3, pp. 923–933, May 2019.
- [15] T.-M. Nguyen, Z. Qiu, M. Cao, T. H. Nguyen, and L. Xie, "Single landmark distance-based navigation," *IEEE Transactions on Control Systems Technology*, 2019.
- [16] M. Deghat, I. Shames, B. D. O. Anderson, and C. Yu, "Localization and circumnavigation of a slowly moving target using bearing measurements," *IEEE Transactions on Automatic Control*, vol. 59, no. 8, pp. 2182–2188, 2014.
- [17] R. Zheng, Y. Liu, and D. Sun, "Enclosing a target by nonholonomic mobile robots with bearing-only measurements," *Automatica*, vol. 53, pp. 400–407, 2015.
- [18] J. Hu, L. Xie, and C. Zhang, "Energy-based multiple target localization and pursuit in mobile sensor networks," *IEEE Transactions on Instrumentation & Measurement*, vol. 61, no. 1, pp. 212–220, 2011.
- [19] G. Chai, C. Lin, Z. Lin, and W. Zhang, "Consensus-based cooperative source localization of multi-agent systems with sampled range measurements," *Unmanned Systems*, vol. 2, no. 03, pp. 231–241, 2014.
- [20] M. Zhang and H. H. T. Liu, "Vision-based tracking and estimation of ground moving target using unmanned aerial vehicle," in *American Control Conference*, 2010, pp. 6968–6973.
- [21] D. Milutinović, D. Casbeer, Y. Cao, and D. Kingston, "Coordinate frame free Dubins vehicle circumnavigation," in *American Control Conference*, 2014, pp. 891–896.
- [22] —, "Coordinate frame free Dubins vehicle circumnavigation using only range-based measurements," *International Journal of Robust & Nonlinear Control*, vol. 27, no. 16, pp. 2937–2960, 2017.
- [23] Y. Cao, "UAV circumnavigating an unknown target under a GPS-denied environment with range-only measurements," *Automatica*, vol. 55, pp. 150–158, 2015.
- [24] M. Zhang, P. Tian, and X. Chen, "Unmanned aerial vehicle guidance law for ground target circumnavigation using range-based measurements," *International Journal of Control Automation & Systems*, vol. 15, no. 5, pp. 2455–2460, 2017.
- [25] A. S. Matveev and A. A. Semakova, "Range-only-based three-dimensional circumnavigation of multiple moving targets by a nonholonomic mobile robot," *IEEE Transactions on Automatic Control*, vol. 63, no. 7, pp. 2032–2045, 2017.
- [26] A. S. Matveev, A. A. Semakova, and A. V. Savkin, "Tight circumnavigation of multiple moving targets based on a new method of tracking environmental boundaries," *Automatica*, vol. 79, pp. 52–60, 2017.
- [27] A. S. Matveev, H. Teimoori, and A. V. Savkin, "Method for tracking of environmental level sets by a unicycle-like vehicle," *Automatica*, vol. 48, no. 9, pp. 2252–2261, 2012.
- [28] R. P. Anderson and D. Milutinovic, "A stochastic approach to dubins vehicle tracking problems," *IEEE Transactions on Automatic Control*, vol. 59, no. 10, pp. 2801–2806, 2014.
- [29] S. Guler and B. Fidan, "Range based target capture and station keeping of nonholonomic vehicles without GPS," in *European Control Conference*, 2015, pp. 2970–2975.
- [30] J. Lin, S. Song, K. You, and C. Wu, "3-D velocity regulation for nonholonomic source seeking without position measurement," *IEEE Transactions on Control Systems Technology*, vol. 24, no. 2, pp. 711–718, 2016.
- [31] J. A. Moreno and M. A. Osorio, "A Lyapunov approach to second-order sliding mode controllers and observers," in *IEEE Conference on Decision and Control*, 2009, pp. 2856–2861.
- [32] J. O. Swartling, I. Shames, K. H. Johansson, and D. V. Dimarogonas, "Collective circumnavigation," *Unmanned Systems*, vol. 2, no. 03, pp. 219–229, 2014.
- [33] F. Dong, Y. Hsu, and K. You, "Circumnavigation of an unknown target using range-only measurements in GPS-denied environments," in *IEEE International Conference on Control and Automation*, July 2019, pp. 411–416.
- [34] F. Dong, K. You, and S. Song, "Target encirclement with any smooth pattern using only range-based measurements," *arXiv:1906.07416*, 2019.
- [35] H. K. Khalil, *Nonlinear Systems (3rd Ed.)*. Prentice Hall, 2002.
- [36] X. Yu and L. Liu, "Target enclosing and trajectory tracking for a mobile robot with input disturbances," *IEEE Control Systems Letters*, vol. 1, no. 2, pp. 221–226, 2017.
- [37] R. W. Beard and T. W. McLain, *Small Unmanned Aircraft: Theory and Practice*. Princeton University Press, 2012.
- [38] J. Lee, "Small fixed wing UAV simulator," Apr. 2016. [Online]. Available: <https://github.com/magiccjae/ecen674>
- [39] S. H. Strogatz, *Nonlinear Dynamics and Chaos: with Applications to Physics, Biology, Chemistry, and Engineering (2nd Edition)*. Boca Raton: CRC Press, 2018.